Method for spherical camera to 3D LiDAR calibration and synchronization with example on Insta360 X4 and LiVOX MID 360

Janusz Bedkowski[1], Michał Pełka[2], Karol Majek[3], Marcin Matecki[1]

[1] Institute of Fundamental Technological Research, Polish Academy of Science, ul. Pawińskiego 5B, 02–106, Warsaw, Poland, januszbedkowski@gmail.com, matecki.m@outlook.com
[2] Robotec.ai, Warsaw, Poland, michalpelka@gmail.com
[3] Cufix, Grodzisk Mazowiecki, Poland, karolmajek@gmail.com

Keywords: mobile mapping, sensor synchronization, 360 camera, 3D lidar

Abstract

This paper introduces a method for 360 camera with 3D LiDAR calibration and synchronization with example on Insta360 X4 and LiVOX MID 360. Both data streams (camera and LiDAR) are recorded separately to reach interoperability, robustness, full resolution, and maximal FPS (Frames Per Second). The novelty is based on LED circle strip illuminating timestamp, thus this information is recorded by camera. The timestamp is presented using gray code utilizing individually addressed LED strips. The data signal for LED is prepared by micro-controller. Microcontroller (ESP-8285) communicates using USB. We incorporated ResNet-18 based binary classifier to classify LEDs. Our method can efficiently assign timestamps with a resolution of 100 ms. To fulfill the process of 3D point cloud colorization, we implemented camera to LiDAR calibration procedure requiring manually assigning 5 pairs of image to 3D point correspondences. Our method is independent from hardware, thus it can be used also for affordable one making it more accessible and easy to use.

1. Introduction

Image to LiDAR calibration and synchronization are essential for mobile mapping systems. At least in two domains: land survey (14)(15) and aerial survey (16)(17)(18) all sensors are synchronized and calibrated for providing best accuracy and precision according to GPS/GNSS signal. It is possible to improve the accuracy and precision with SLAM (Simultaneous Localization and Mapping) approach (19). Our contribution is based on the problem of building a reliable mobile mapping system made up of affordable sensors. We expect the recording image stream to be in full resolution and with maximal available FPS (frame per second). For example, camera Insta360 X4 can record 8K with 30 FPS, making it great data source for many applications. Furthermore, our 360 LiDAR is based on MANDEYE system (2) that is based on currently most affordable LiDAR LiVOX MID360. We incorporated onboard computer Raspbery PI 4B, thus it required incorporating novel approach to data synchronization based on additional LED strip coding timestamps.

Indoor mapping (1) of shopping molls, train stations, metro, university hall, hospitals, airports is not anymore considered as technological challenge (2). Most of commercially available devices are hand held, backpacks and trolleys equipped with LiDARs, cameras, IMU and other sensors helping with trajectory estimation (3)(4). The challenge is georeferencing of indoor map since it requires an additional effort for fusing e.g. GCP (Ground Control Points). This drawback requires highly specialized personnel for data collection and processing. Surroundings of the building (5) such as gardens(7), forest (6), road infrastructure(7) and pedestrian area(7) can be surveyed with the same equipment. Mobile mapping system is typically equipped with accurate GNSS receiver with RTK such as mobile robots (8). This modality is considered by plenty of mobile mapping systems, expensive and affordable ones. Thus, it has largest impact into mobile mapping adoption in Forensic and Security. Not so many challenges can be identified here. Problems appears in outdoor-indoor transition e.g. entering zone under bridge etc.. where there is limited access to GNSS signal. The drawback is related with heavy backpack mobile mapping system that determines fatigue. Moreover, the backpack solution limits mobility in tiny spaces.

Most of precise 3D measurement tools(9) are applied for small scale surveys. E.g. close range photogrammetry can be applied for this scenario (10)(11). Also iPhone LiDAR can be applied here (12). Or many other mapping systems (13) capable acquiring precise 3D data in short distance. The survey can be done also with backpack mobile mapping systems (20) and hand held devices. Useful functionality is a layout generation (21)(22) as a very promising tool for creating digital twins. Mmobile mapping systems are widely used in underground surveys (23). The challenge is luck of GNSS signal, thus the transition into large scale domains requires other techniques of georeferencing. It can be seen that this particular domain is well covered by different types of mobile mapping systems.

Affordable virtual reality content acquisition and viewing in head-mounted virtual reality(24) is one of our main goals. Recent work on CNNs shows grate potential e.g. for generating 360-degree high-quality, spatio-temporally coherent human videos from a single image (25). To conclude, the commercialization of Virtual Reality (VR) headsets has made immersive and 360-degree video streaming the subject of intense interest in the industry and research communities (26). Based on literature search we claim that our contribution is as follows:

- affordable open source mobile mapping system with synchronized 360 camera,
- capability to record and to synchronize (off-line) 8K 360 camera stream at 30fps (LiDAR and 360 camera streams are recorded on separate memory cards),

- open source software for 360 camera to LiDAR calibration,
- we provided all necessary software components as a part of an open source project `https://github.com/MapsHD/HDMapping`.

2. 360 camera to LiDAR calibration

2.1 Hardware

We improved handheld mobile mapping system (2) (see figure 1) by adding camera Insta360 X4 and ring of LEDs (see figure 2). This setup enables collecting 8K video with 30fps. Ring of LEDs enables coding timestamp with Grey code, thus it is possible to synchronized LiDAR and camera streams with 100ms resolution.

Figure 1. MANDEYE-DEV system composed of LiDAR MID360 and camera Insta360 X4.

2.2 Colinearity observation equation

To build equirectangular camera colinearity observations first we use the *camera←world* $[R,t]_{cw}$ matrix that transforms 3D point $P^g(x^g, y^g, z^g, 1)$ in global reference system to point $P^l(x^l, y^l, z^l)$ in local camera reference system. The idea of transforming spherical coordinates into equirectangular image is shown in figure (3)).

$$P^l = [R,t]_{cw} P^g = [R,t]_{wc}^{-1} P^g \tag{1}$$

Secondly, we move point $P^l(x^l, y^l, z^l)$ to the sphere with radius equals 1 ($P^l_{r=0}$).

$$P^l = \begin{bmatrix} p^l_x \\ p^l_y \\ p^l_z \end{bmatrix} \tag{2}$$

$$\left\| P^l \right\| = \sqrt{{p^l_x}^2 + {p^l_y}^2 + {p^l_z}^2} \tag{3}$$

$$P^l_{r=0} = \begin{bmatrix} \frac{p^l_x}{\left\| P^l \right\|} \\ \frac{p^l_y}{\left\| P^l \right\|} \\ \frac{p^l_z}{\left\| P^l \right\|} \end{bmatrix} \tag{4}$$

Figure 2. Zoom to LED strips. Our system is capable classifying this LEDs and decode timestamps assigned by onboard computer.

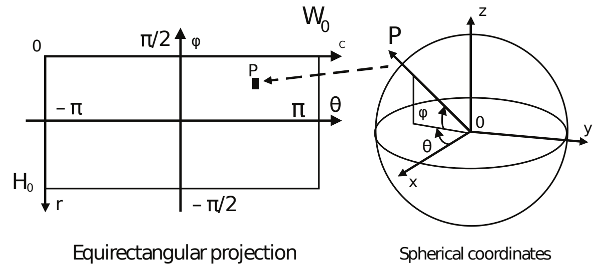

Figure 3. Transforming spherical coordinates into equirectangular image in photogrammetry.

Having image sizes [cols, rows], the coordinates on the image sphere can be derived from:

$$\begin{bmatrix} latitude \\ longitude \end{bmatrix} = \begin{bmatrix} -asin(\frac{p^l_y}{\left\| P^l \right\|}) \\ atan(\frac{\frac{p^l_x}{\left\| P^l \right\|}}{\frac{p^l_z}{\left\| P^l \right\|}}) \end{bmatrix} \tag{5}$$

Finally, $\Psi_{[[R,t]_{wc}, x^g, y^g, z^g]}$ function is given:

$$\Psi_{[\beta]} = \begin{bmatrix} u \\ v \end{bmatrix} = \begin{bmatrix} cols(0.5 + \frac{lon}{2\pi}) \\ rows(0.5 - \frac{lat}{\pi}) \end{bmatrix} \tag{6}$$

where $\beta = \left[[R,t]_{wc}, x^g, y^g, z^g\right]$ is set of unknowns (parameterized rotation $[R,t]$ and coordinates of a terrain point x^g, y^g, z^g) to be calculated during calibration. It is worth mentioning that x^g, y^g, z^g are derived from LiDAR data (by manual picking) and are considered as constant values. To build the observation equation incorporating the projection of point $P^g(x^g, y^g, z^g)$ onto image sphere (r=1) the following optimization problem is considered:

$$\min_{[R,t]_{wc}} \sum_{i=1}^{C} \left(\left[u^{kp}, v^{kp}\right]^{-} \Psi_{[\beta]}([R,t]_{wc}, x^g, y^g, z^g) \right)^2 \tag{7}$$

where there are C projections $[u, v]$ of points (x_i^g, y_i^g, z_i^g) onto image sphere. Thus, equirectangular camera colinearity observation equation is given in (8),

$$\boxed{\underbrace{\begin{bmatrix} u_\delta \\ v_\delta \end{bmatrix}}_{residuals} = \underbrace{\begin{bmatrix} u^{kp} \\ v^{kp} \end{bmatrix}}_{target\ values} - \underbrace{\Psi_{[\beta]}([R,t]_{wc}, x^g, y^g, z^g)}_{model\ function}} \quad (8)$$

where $\begin{bmatrix} u_\delta \\ v_\delta \end{bmatrix}$ are *residuals*, $\begin{bmatrix} u^{kp} \\ v^{kp} \end{bmatrix}$ are *target values* and $\Psi_{[[R,t]_{wc}, x^g, y^g, z^g]}([R,t]_{wc}, x^g, y^g, z^g)$ is the *model function*.

2.3 Open source camera to LiDAR calibration software

We provided an open source software (Figure 4) available at `https://github.com/MapsHD/HDMapping` (name: mandeye_with_360_camera_manual_coloring). End user should pick at least five image-LiDAR pairs to conduct calibration. Final calibration matrix is stored in .json file.

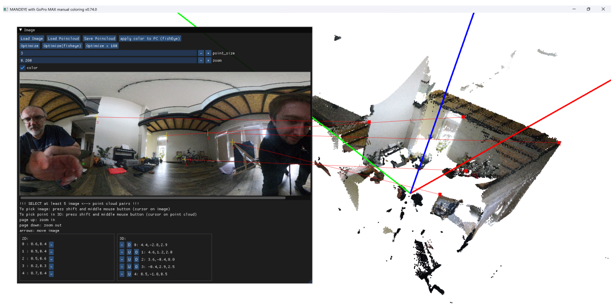

Figure 4. Colored point cloud with the open source software available at `https://github.com/MapsHD/HDMapping`.

2.4 Synchronization processing pipeline

The timestamp is presented using gray code utilizing individually addressed LED strips. Data signal for LED is prepared by micro-controller. Micro-controller (ESP-8285) communicates with MANDEYE-DEV mobile mapping system using USB. Its firmware is created using Arduino and utilizes FastLED library and Arduino JSON library code. On Mandeye device a C++ program is run that has a ZMQ subscriber. Subscriber receives timestamp and state of the device. That is packed to JSON and sent through USB to the Microcontroller. USB is used to power the LED strip and the microcontroller. Figures 5-12 show our processing pipeline to achieve cropped little planet projection of equirectangular image for improved detection capability and Hough circles detection performance on CIELAB color space 2nd channel.

Figures 13-16 show detection-less approach with ResNet-18 based binary classifier. Figure 17 shows a timestamps automatically classified with ResNet-18 binary classifier (White box - LED not active, red box - LED active).

3. Synchronization experiment

Figure 17 shows plot of timestamps automatically classified with ResNet-18 binary classifier. Figures 13,14 show correct LEDs' classification. Figure 15 shows classification errors - poor generalization. Our experiment shows that neural network fails sometimes. For this reason we approximate final result (see figure 17), thus we can retrieve time stamp for each 360 frame. Our solution provides point cloud, trajectory, 360 images. Each 360 image has assigned timestamp to the node of the trajectory. The resolution of our timestamp is 100ms.

Figure 5. Original equirectangular image

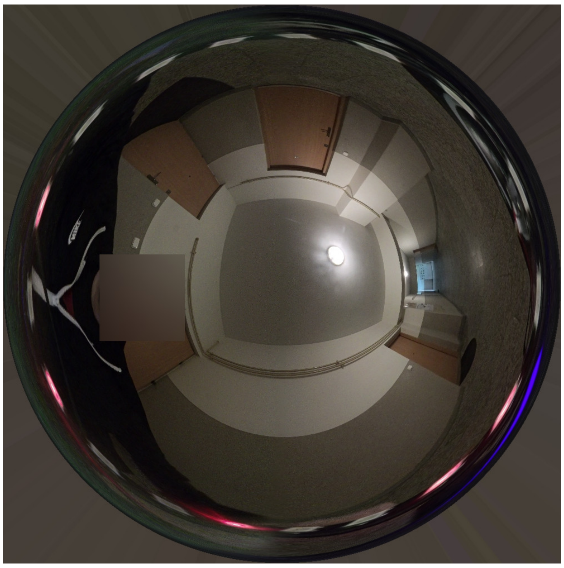

Figure 6. Little planet projection

4. Coloring experiment

We performed and an experiment of coloring 3D point cloud with data derived from 360 camera. For this purpose we collected 10 stationary scans in different locations. We registered them with our software. First camera to LiDAR data was calibrated with provided software and the calibration matrix was applied for all 10 stations. Final result is shown in figure 18. Zoomed view is shown in figure 19.

5. Summary

We built camera to LiDAR calibration working prototype. We prepared an open-source open hardware documentation so that everyone can benefit from our contribution. We performed successful experiment of colorizing session recoded with MANDEYE mobile mapping system. Our synchronization method can efficiently assign timestamp for each 360 image. This timestamp is provided by LiDAR, thus all sensors can benefit from it. Unfortunately, entire procedure is offline. Based on our best knowledge our system is most affordable that

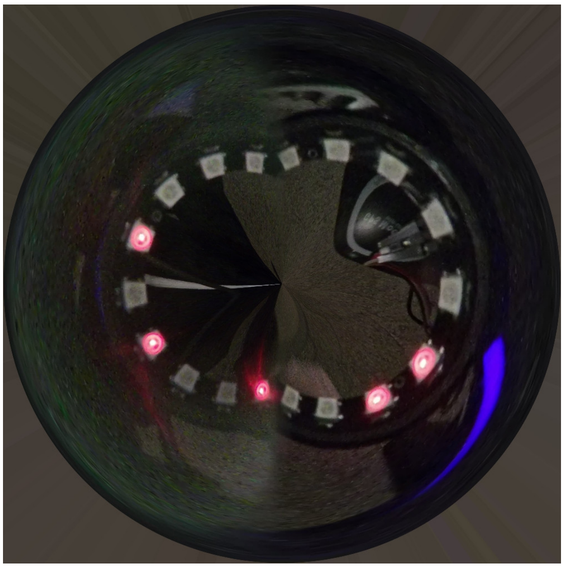

Figure 7. Projection of 20% image height

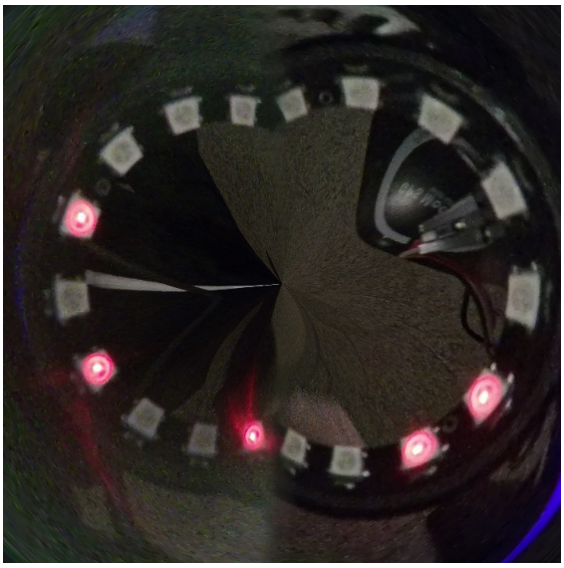

Figure 8. Cropped projection for automatic detection

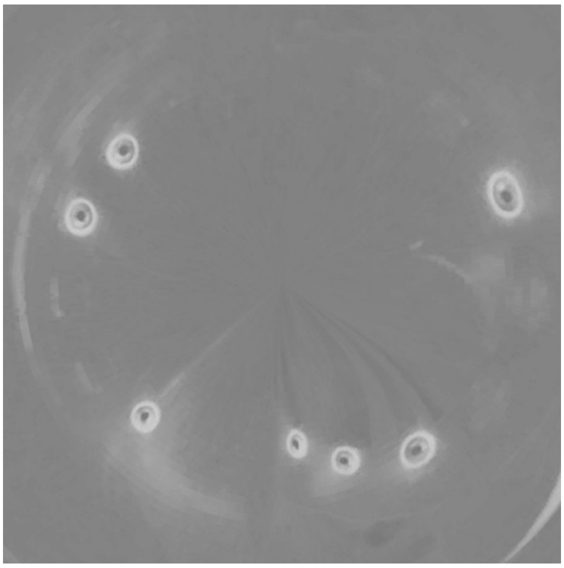

Figure 9. CIELAB color space 2nd channel

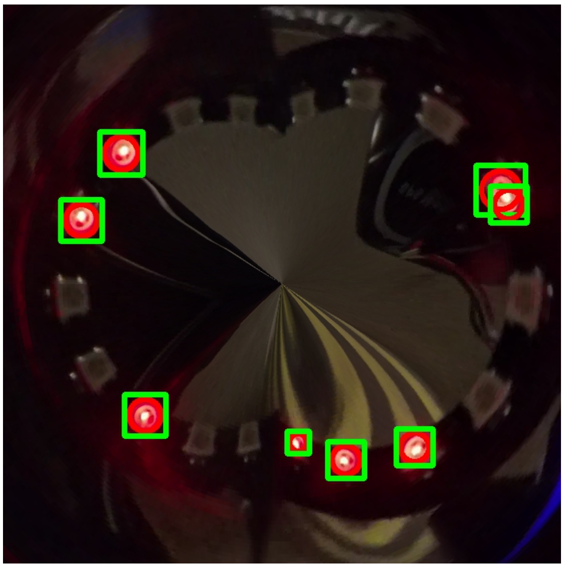

Figure 10. Visualization of Hough circle detections

can provide 8K 360 images at 30fps. It is possible that our solution is compatible with most of a consumer grade 360 cameras. Our solution can help in LiDAR/360 data collection and organization in large scale surveys even when we use customer grade equipment. In our opinion there are plenty of potential applications since mobile mapping systems are already widely adopted in plenty domains.

6. Future work

Most significant drawback of our solution is the complexity of the procedure. We are going to automatize the colorizing step, thus overall pipeline will be simplified. The resolution of our timestamp is 100ms, thus it is difficult at this stage of the development to accurately colorize data acquired during motion. For this purpose we are going to investigate such a method.

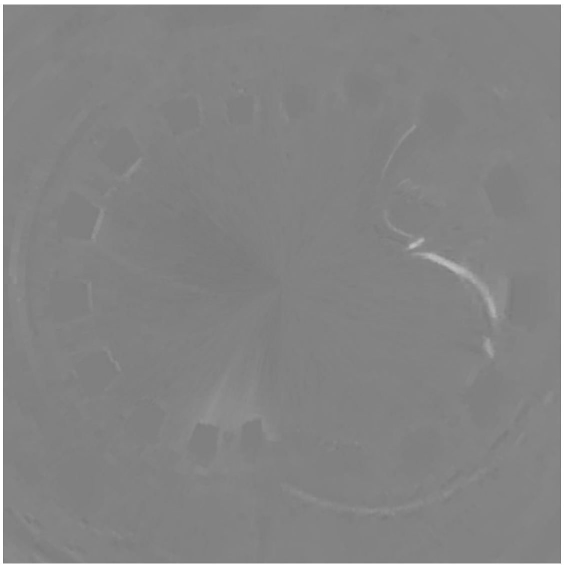

Figure 11. CIELAB 2nd channel - overexposed

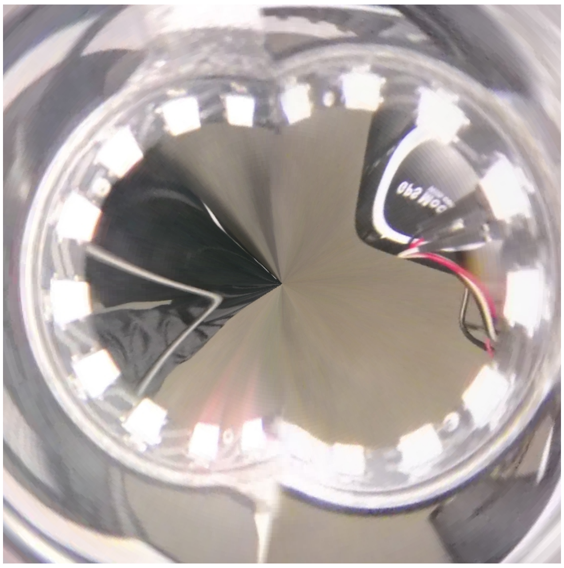

Figure 12. Hough circle detections - overexposed. Equirectangular image processing pipeline to achieve cropped little planet projection for improved detection capability. Hough circles detection performance on CIELAB color space 2nd channel.

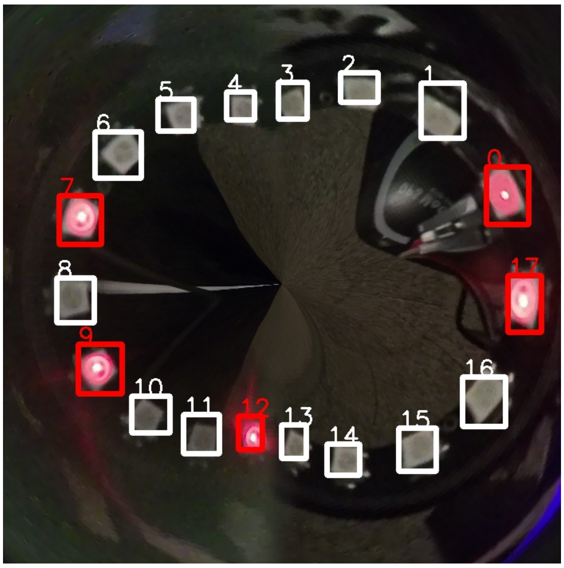

Figure 13. Example result, correct classification

Figure 14. Example result, correct classification

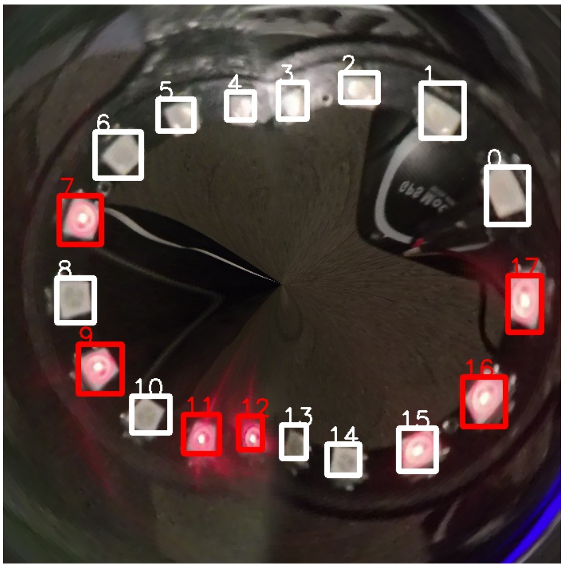

Figure 15. Classification errors - poor generalization. Detection-less approach with ResNet-18 based binary classifier. White box - LED not active, red box - LED active.

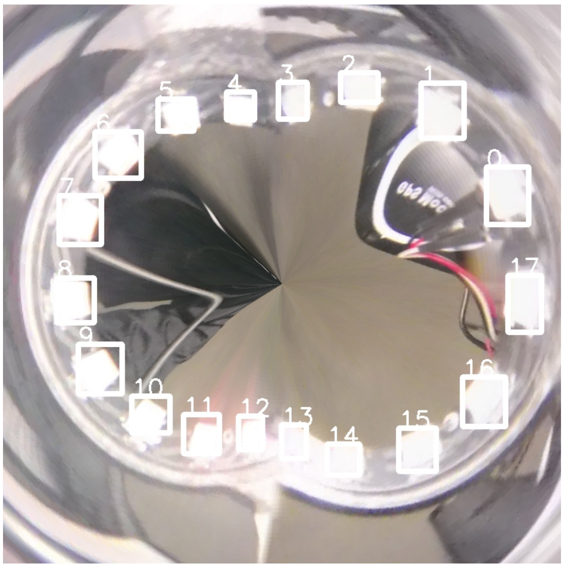

Figure 16. Detection error due to lighting conditions. Detection-less approach with ResNet-18 based binary classifier. White box - LED not active, red box - LED active.

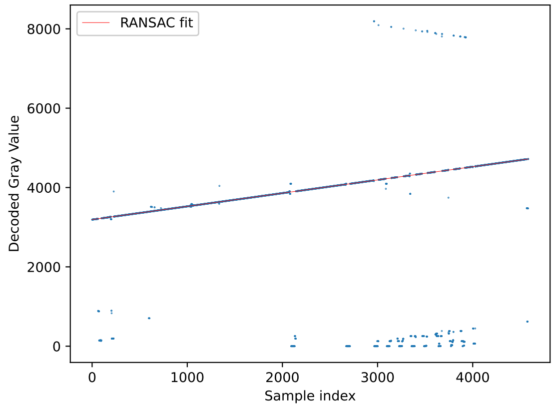

Figure 17. Plot of timestamps automatically classified with ResNet-18 binary classifier.

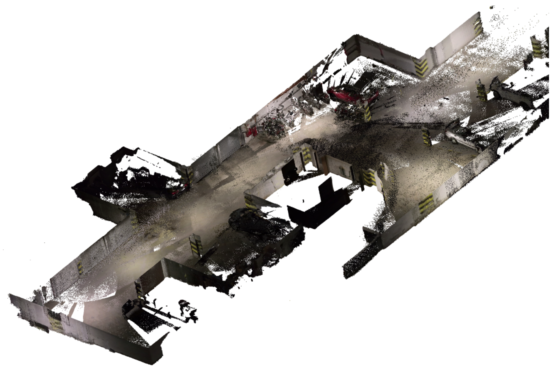

Figure 18. Colored point cloud of the underground garage. We collected 10 stationary scans in different locations. We registered them with our software. First camera to LiDAR data was calibrated with provided software and the calibration matrix was applied for all 10 stations.

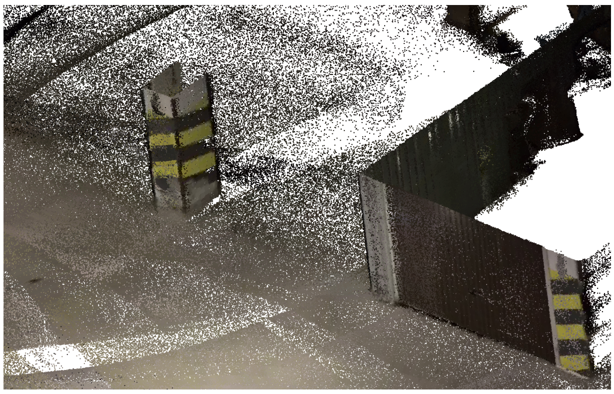

Figure 19. Zoomed colored point cloud of the underground garage.

References

R. Otero, S. Lagüela, I. Garrido, P. Arias ”Mobile indoor mapping technologies: A review”, Automation in Construction Volume 120, December 2020, 103399

J. Bedkowski ”Open source, open hardware hand-held mobile mapping system for large scale surveys”, SoftwareX Volume 25, February 2024, 101618

J. Kaltenthaler, H. A. Lauterbach, D. Borrmann, A. Nüchter ”Pose estimation and mapping based on IMU and LiDAR”, IFAC-PapersOnLine Volume 55, Issue 8, 2022, Pages 71-76

V. Kubelka, M. Reinstein, T. Svoboda ”Improving multimodal data fusion for mobile robots by trajectory smoothing”, Robotics and Autonomous Systems Volume 84, October 2016, Pages 88-96

E. Maset, S. Cucchiaro, F. Cazorzi, F. Crosilla, A. Fusiello, A. Beinat ”Investigating the performance of a hanheld mobile mapping system in different outdoor scenarios”, The International Archives of the Photogrammetry, Remote Sensing and Spatial Information Sciences, Volume XLIII-B1-2021 XXIV ISPRS Congress (2021 edition)

F. Fassi, L. Perfetti ”Backpack mobile mapping solution for DTM extraction of large inaccesible spaces”, The International Archives of the Photogrammetry, Remote Sensing and Spatial Information Sciences, Volume XLII-2/W15, 2019 27th CIPA International Symposium “Documenting the past for a better future”, 1–5 September 2019, Ávila, Spain

P. Yu, M. Wang and H. Chen ”Integration and evaluation of SLAM-based backpack mobile mapping system”, E3S Web of Conferences 206, 03014 (2020), ICGEC 2020

T. Jilek ”Autonomous field measurement in outdoor areas using a mobile robot with RTK GNSS”, IFAC-PapersOnLine 48-4 (2015) 480–485

F. M. Sheshtar, W. M. Alhatlani, M. Moulden and J. Hyuk Kim ”Comparative Analysis of LiDAR and Photogrammetry for 3D Crime Scene Reconstruction”, Appl. Sci. 2025, 15, 1085

M. Salado Puerto, H. Tullerb ”Large-scale forensic investigations into the missing: Challenges and considerations”, Forensic Science International 279 (2017), 219-228

R.M. Carew et al. ”3D forensic science: A new field integrating 3D imaging and 3D printing in crime reconstruction”, Forensic Science International: Synergy 3 (2021) 100205

S. Kottner, M. J. Thali, D. Gascho,”Using the iPhone’s LiDAR technology to capture 3D forensic data at crime and crash scenes”, Forensic Imaging 32 (2023) 200535

S. Natalia, K. Iwona, O. Kinga, B. Krzysztof ”Towards development of mobile mapping systems, Archiwum Fotogrametrii, Kartografii i Teledetekcji, Zarzad Głowny Stowarzyszenia Geodetów Polskich, vol. 35, 2023, pp. 85-105

Z. Shena, J. Wanga, C. Panga, Z. Lana, Z. Fanga ”A LiDAR-IMU-GNSS fused mapping method for large-scale and high-speed scenarios”, Measurement Volume 225, 15 February 2024, 113961

A. Ferraz, C. Mallet, N. Chehata ”Large-scale road detection in forested mountainous areas using airborne topographic lidar data”, ISPRS Journal of Photogrammetry and Remote Sensing Volume 112, February 2016, Pages 23-36

G. Lenda, U. Marmol ”Integration of high-precision UAV laser scanning and terrestrial scanning measurements for determining the shape of a water tower”, Measurement Volume 218, 15 August 2023, 113178

K. Kuželka, M. Slavík and P. Surový ”Very High Density Point Clouds from UAV Laser Scanning for Automatic Tree Stem Detection and Direct Diameter Measurement”, Remote Sens. 2020, 12(8)

L. Gu, H. Zhang, X. Wu, Surveying and mapping of large-scale 3D digital topographic map based on oblique photography technology, Journal of Radiation Research and Applied Sciences Volume 17, Issue 1, March 2024, 100772

Bedkowski J, Nowak H, Kubiak B, Studzinski W, Janeczek M, Karas S, Kopaczewski A, Makosiej P, Koszuk J, Pec M, et al. A Novel Approach to Global Positioning System Accuracy Assessment, Verified on LiDAR Alignment of One Million Kilometers at a Continent Scale, as a Foundation for Autonomous DRIVING Safety Analysis. Sensors. 2021; 21(17):5691. https://doi.org/10.3390/s21175691

H. A. Lauterbach, D. Borrmann, R. Heß, D. Eck, K. Schilling and A. Nüchter ”Evaluation of a Backpack-Mounted 3D Mobile Scanning System”, Remote Sens. 2015, 7(10), 13753-13781

S. Karam, G. Vosselman, M. Peter, S. Hosseinyalamdary and V. Lehtola ”Design, Calibration, and Evaluation of a Backpack Indoor Mobile Mapping System”, Remote Sens. 2019, 11(8), 905

R. E. Weber, C. Mueller, C. Reinhart ”Automated floorplan generation in architectural design: A review of methods and applications”, Automation in Construction Volume 140, August 2022, 104385

J. Wang, L. Wang, P. Peng, Y. Jiang, J. Wu, Y. Liu ”Efficient and accurate mapping method of underground metal mines using mobile mining equipment and solid-state lidar”, Measurement Volume 221, 15 November 2023, 113581

Wen-Chih Lo, Ching-Ling Fan, Jean Lee, Chun-Ying Huang, Kuan-Ta Chen, and Cheng-Hsin Hsu. 2017. 360° Video Viewing Dataset in Head-Mounted Virtual Reality. In Proceedings of the 8th ACM on Multimedia Systems Conference (MMSys’17). Association for Computing Machinery, New York, NY, USA, 211–216. https://doi.org/10.1145/3083187.3083219

Ruizhi Shao, Youxin Pang, Zerong Zheng, Jingxiang Sun, Yebin Liu, Human4DiT: 360-degree Human Video Generation with 4D Diffusion Transformer, https://arxiv.org/abs/2405.17405, 2024

Federico Chiariotti, A survey on 360-degree video: Coding, quality of experience and streaming, Computer Communications, Volume 177, 2021, Pages 133-155, ISSN 0140-3664, https://doi.org/10.1016/j.comcom.2021.06.029.